energies

MDPI

Article

Abnormal Phenomena and Mathematical Model of Fluid Imbibition in a Capillary Tube

Wenquan Deng, Tianbo Liang *, Shuai Yuan, Fujian Zhou and Junjian Li

State Key Laboratory of Oil and Gas Resources and Prospecting, China University of Petroleum at Beijing, Beijing 102249, China; dwq10284413@163.com (W.D.); yuanshuai_2015@163.com (S.Y.); zhoufj@cup.edu.cn (F.Z.); junjian@cup.edu.cn (J.L.)

* Correspondence: liangtianboo@163.com

Abstract: At present, the imbibition behavior in tight rocks has been attracted increasing attention since spontaneous imbibition plays an important role in unconventional oil and gas development, such as increasing swept area and enhancing recovery rate. However, it is difficult to describe the imbibition behavior through imbibition experiment using tight rock core. To characterize the imbibition behavior, imbibition and drainage experiments were conducted among water, oil, and gas phases in a visible circular capillary tube. The whole imbibition process is monitored using a microfluidic platform equipped with a high frame rate camera. This study conducts two main imbibition experiments, namely liquid-displacing-air and water-displacing-oil experiments. The latter is a spontaneous imbibition that the lower-viscosity liquid displaces the higher-viscosity liquid. For the latter, the tendency of imbibition rate with time does not match with previous model. The experimental results indicate that it is unreasonable to take no account of the effect of accumulated liquid flowing out of the capillary tube on imbibition, especially in the imbibition experiments where the lower-viscosity liquid displaces the higher-viscosity liquid. A mathematical model is established by introducing an additional force to describe the imbibition behavior in capillary tube, and the model shows a good prediction effect on the tendency of imbibition rate with time. This study discovers and analyzes the effect of additional force on imbibition, and the analysis has significances to understand the imbibition behavior in tight rocks.

Keywords: spontaneous imbibition; hydraulic fracturing; microfluidics; tight rock

Citation: Deng, W.; Liang, T.; Yuan, S.; Zhou, F.; Li, J. Abnormal Phenomena and Mathematical Model of Fluid Imbibition in a Capillary Tube. *Energies* **2022**, *15*, 4994. https://doi.org/10.3390/en15144994

Academic Editor: Daoyi Zhu

Received: 22 May 2022
Accepted: 5 July 2022
Published: 8 July 2022

1. Introduction

At present, horizontal wells and hydraulic fracturing are two key technologies for developing tight oil and gas reservoirs [1,2]. However, due to both fast water breakthrough and production decline, the recovery rate of oil and gas is typically less than 10% [3,4]. In tight rocks, the imbibition behavior is strongly affected by the capillary force, where the pore throat size is less than 1 μm [5], and improving water imbibition in fracture and porous matrix can enhance the recovery rate after fracturing. In order to predict oil and water flow in small pores, it is necessary to establish a numerical solution of imbibition rate in the regular-shaped visual model, which considers the influence of viscosity, interfacial tension, and pore diameter on imbibition rate.

Imbibition behavior and its factors through laboratory experiments using single channels have been studied for a long time. Mathematical models have been proposed to describe the imbibition behavior, among which the most classical formulas are Washburn equation and Poiseuille equation [6]. As early as 1921, Lucas (1918) [7] and Washburn (1921) [8] mathematically described the capillary phenomenon in a vertically placed circular tube. In this study, the tube diameter was small enough to ignore the influence of gravity, and the Washburn equation was obtained on basis of Poiseuille equation under the condition that only viscous and capillary forces were considered. Similarly, the equation

is consistent with that in a horizontal single channel. Washburn equation and Poiseuille equation are respectively shown as Equations (1) and (2).

$$L^2 = \frac{R\sigma \cdot cos\theta}{2\mu} \cdot t \tag{1}$$

$$q = \frac{\pi R^4 \Delta P}{8\mu \Delta L} \tag{2}$$

Therein, R represents radius of circular single channel; μ indicates the liquid viscosity; L represents the imbibition distance at the corresponding imbibition time t; θ is the contact angle; σ indicates surface tension; q denotes volume rate of flow; $\Delta P/\Delta L$ represents pressure gradient along the direction of the circular single channel.

Equation (1) not only shows a linear relationship between the imbibition distance and the square root of time, but also gives an idea to establish a mathematical model which describes the imbibition behavior that one liquid displaces another liquid. In the liquid-liquid imbibition, viscous force comes from the flow of displacing phase and displaced phase. Considering an extra applied pressure drop, Poiseuille mathematical model for liquid-liquid imbibition is shown as Equation (3) [6].

$$\frac{1}{8}\left(P_c + \Delta P_{applied}\right) \cdot R^2 t = \frac{1}{2}(\mu_w - \mu_{nw})L^2 + \mu_{nw} \cdot L_{channel} \cdot L \tag{3}$$

Therein, P_c represents capillary force; $\Delta P_{applied}$ indicates an extra applied pressure drop; μ_w and μ_{nw} represent the viscosity of wetting phase and non-wetting phase respectively; $L_{channel}$ is the length of circular single channel.

As shown in Equation (3), general studies of displacement in artificial core or micro model were conducted in the context that an extra pressure drop is applied [9,10]. However, spontaneous imbibition, which refers to the wetting phase flowing spontaneously into the porous media or single channel and displacing the non-wetting phase only by the capillary force [11], does not consider the extra pressure. Therefore, Equation (3) becomes Equation (4) after introducing the equation of capillary force.

$$\frac{\sigma R cos\theta}{4} t = \frac{1}{2}(\mu_w - \mu_{nw})L^2 + \mu_{nw} \cdot L_{channel} \cdot L \tag{4}$$

Equation (4) shows that the imbibition distance as a function of time is mainly related to the length and diameter of the single channel, contact angle, interfacial tension and wettability [12,13]. Wang et al. (2019) [12] proposed a semi-analytical mathematical model characterizing co-current spontaneous imbibition that water imbibes into oil-saturated tight sandstone, and found that the larger the maximum pore radius is, the higher the initial imbibition rate is.

Since this semi-analytical mathematical model is established on basis of a circular capillary tube model, the effect of radius on the imbibition rate is same to that in single-channel model. Hilpert (2009a; 2009b) [14,15] derived semi-analytical solutions to liquid imbibition into horizontal and inclined tubes which considers the dynamic contact angle based on the power law and series models, and these two semi-analytical solutions considered the gravity of liquid due to the large diameter of the circular tube.

Soares et al. (2005) [16] found that an uncertainty of contact angle in imbibition studies since the displaced liquid can stick to the capillary-tube wall and consequently influences contact angle during this imbibition process. The uncertainty of contact angle on process of imbibition is also related to interfacial tension [17,18]. Thus, the contact angle (which is influenced by the above factors) is likely to affect imbibition rate, but it does not affect the law of imbibition rate with time. In imbibition studies characterizing mathematically imbibition rate, experiments have generally been conducted in rectangular single channels due to the limit of etching techniques [19–21]. Therefore, in the imbibition experiment of rectangular single channels, the focus is how the length and width of the rectangular single

channel influence the imbibition rate. The researchers developed different mathematical models based on their own experiments to characterize imbibition behavior in rectangular single channels with different sizes [21,22]. Yang et al. (2011, 2014) [23,24] studied the dynamics of capillary-driven flow in open hydrophilic microchannels, and found that the imbibition rate decreases with the increase of channel width. Chen (2014) [25] investigated the penetration of a wetting liquid into open metallic grooves and found that the imbibition rate is faster in deeper grooves. These basic studies provide a better understanding of different factors on imbibition behavior. However, an interesting and unconventional phenomenon was found in the study of Yang et al. (2014). When the lower-viscosity Deionized water (DI-water) displaces the higher-viscosity hexadecane, the imbibition rate shows a decreasing trend with time. This observation is contradictory to the trend proposed by Equation (4), and this is due to the effect of displaced phase on imbibition in single channel was not comprehensively considered.

In this study, imbibition and drainage experiments are conducted among water, oil and gas phases to understand the law of imbibition rate and evaluate the prediction effect of Washburn model and modified Poiseuille model. For imbibition experiment of water-displacing-oil, we modified the Poiseuille model and established this modified Poiseuille model on basis of Equation (4) by introducing a third force come from the reverse imbibition. This modified model explains the effect of displaced liquid that is displaced from single channel on the abnormal phenomenon in imbibition of liquid-displacing-liquid, and it also reveals a new concept that an additional force exists due to reverse imbibition outside the single channel when the lower-viscosity fluid displaces the higher-viscosity fluid. Furthermore, this study provides enlightenment for the analysis of the force during imbibition process in tight rocks.

2. Materials and Methods

2.1. Experimental Materials and Equipment

BZY-2 automatic interface tensioner is used for measuring the interfacial tension through the lifting-ring method. JY-PHB contact angle tester is used for the measurement of contact angle. The imbibition distance as a function of time were monitored using a microfluidic platform equipped with a fluorescent stereo microscope (Leica M165 FC), as shown in Figure 1.

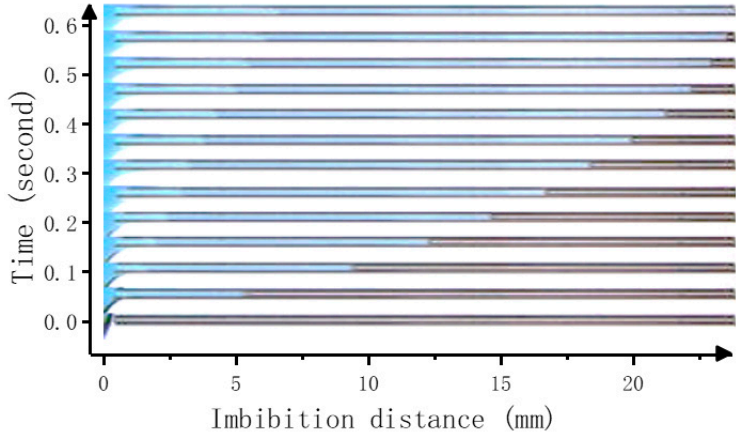

Figure 1. Imbibition that DI-water displaces air in one single channel.

The single-channel models of circular capillary tube used in this paper, which are made of fused silica, are 100 mm in length and 0.3, 0.4, 0.5, and 0.6 mm in the inner diameter. The single-channel models are hydrophilic, and different lengths can be designed for the single-channel model to explore the imbibition effect under different sizes.

The oil sample used is kerosene (from Chengdu Xinzhengtong Chemical Co., Ltd., Chengdu, China). Compared with other oil samples, kerosene does not affect the wettability

of the channel wall during the spontaneous imbibition. The water phase is DI-water, which reduces the influence of impurities on spontaneous imbibition process.

2.2. Experimental Methods

Basic parameters are shown in Table 1. As shown in Table 1, the fluctuation of the contact angle between liquid (DI-water: 79.8° or kerosene: 67°) and air does not apparently influence its cosine. Besides, the contact angles in different tube diameters between liquid and air are almost the same with fluctuation less than 1.5°. However, in the experiment of DI-water-displacing-kerosene, with the range 82.3° to 87.9° of the contact angle between kerosene and DI-water in single channels with three different diameters. Although just ±1° fluctuation of contact angel occurs, greater changes are induced in the corresponding cosine, resulting in influence on the analysis of fitting. Accordingly, the four contact angles are not averaged.

Table 1. Property parameters.

Property	Value	
Viscosity of DI-water	1.0 mPa·s	
Viscosity of kerosene	2.2 mPa·s	
Surface tension between DI-water and air	66.5 mN/m	
Surface tension between kerosene and air	24.0 mN/m	
Interfacial tension between kerosene and DI-water	20.9 mN/m	
The contact Angle between DI-water and air in the single channel	79.8 ± 1.4°	
The contact Angle between kerosene and air in the single channel	67.0° ± 1.2	
The contact Angle between kerosene and DI-water in the single channel	0.3 × 10.60 mm	87.9°
	0.5 × 15.00 mm	86.2°
	0.5 × 19.25 mm	83.5°
	0.6 × 20.67 mm	82.3°

Imbibition experiment of liquid-displacing-air in a single channel: Single-channel models with different diameters in the original water-wet state are selected. After water (or oil) is filtered and dropped on one side of the single channel, the change of water front within the channel is monitored by a Leica M165FC stereo fluorescence microscope at the frame rate of 18 frames per second. The imbibition distance is then plotted versus the time, from which the change of imbibition rate is accordingly observed. When water displaces air, the diameter of the single channel remains constant, while the length is changed for comparison; when oil displaces air, the length of the single channel remains unchanged, but the diameter of the channel is changed for comparison.

Imbibition experiment of water-displacing-oil in a single channel: Single channels with different tube diameters and lengths are selected for imbibition experiments of water-displacing-oil. Under the initial condition of saturated kerosene, the 0.05 mL filtered DI-water droplet is dropped on one side of a single channel, and curves of the imbibition distance as a function of time are obtained by the method above. By comparing experimental results and theoretical models, it is investigated the effects of tube diameter, interfacial tension, and viscosity on the imbibition process.

3. Results and Discussion

3.1. Liquid-Displacing-Air

In imbibition studies, both the Washburn model for imbibition of liquid-displacing-gas and the Poiseuille model for imbibition of liquid-displacing-liquid need to meet the laminar flow condition, and the following steps are intended to determine the flow state of this study.

The determination expression of laminar flow is shown as Equation (5) [26]:

$$R_e = \frac{\rho v d}{\mu} \tag{5}$$

Therein, R_e represents Reynolds number; ρ denotes liquid density; v represents average velocity; d is diameter of circular single channel; μ indicates the liquid viscosity.

The Equation (5) shows that Reynolds number is relative to ρ, d, μ, and v, and the v is affected by other factors shown as Equation (6) which is derived from Equation (1).

$$v = \sqrt{\frac{R\sigma \cdot cos\theta}{8\mu}} \cdot t^{-0.5} \tag{6}$$

According to the critical Reynolds number of laminar flow, the condition satisfied the laminar flow is $R_e < 2300$. According to Equations (5) and (6), the Reynolds number increases with the increase of density, diameter and interfacial tension, as well as the decrease of viscosity and contact angle. Therefore, the Reynolds number is most likely to break through critical Reynolds number in the imbibition process of water-displacing-air with large-diameter tube. If imbibition experiments of water-displacing-air meet the laminar flow condition, so do that of oil-displacing-air and water-displacing-oil.

It is assumed that imbibition of water-displacing-air occurs in a 0.5 mm single channel, and the Reynolds number is exactly 2300, then the calculated limit imbibition rate is 4.6 m/s. According to Equation (6), the imbibition rate decreases with time, and the time interval when the initial imbibition rate is greater than the limit one is:

$$t < 1.38 \times 10^{-5} \text{ s}$$

This time interval is short enough to identify the flow as laminar.

Based on the analysis above, the imbibition process of liquid-displacing-air is in line with the Washburn model's assumptions so that the Washburn model can be used for analysis of the process, and Poiseuille model may be accordingly utilized for prediction on the imbibition process of water-displacing-oil.

In imbibition experiments of liquid-displacing-air, there is no other force except for capillary force. Moreover, the influence of gravity on a liquid droplet is also insignificant compared with the capillary force. Therefore, the displacement force is considered to come only from capillary force.

The experimental results obtained through the microfluidic platform equipped with a fluorescent stereo microscope (Leica M165 FC) and the corresponding prediction curves obtained from Equation (1) are shown in Figure 2, and results of the imbibition distance as a function of $\sqrt{t}$ are shown in Figure 3.

Figures 2 and 3 show that curves of the imbibition distance as a function of time in imbibition experiments liquid-displacing-air with circular single channels fit well with the Washburn model. In the imbibition process that water (or oil) droplet enters the single channel initially saturated with air, the imbibition rate, which varies with the diameter of single channel, decreases gradually with the increase of imbibition distance, and the imbibition distance is linear with the square root of time. Under the condition that the diameters of single channels are all 0.3 mm, four curves of water-displacing-air fluctuate within an acceptable range, indicating that the length of single channel has no influence on imbibition behavior of liquid-displacing-air to some extent.

According to the imbibition distance as a function of time, the imbibition rate can be determined as shown in Figure 4.

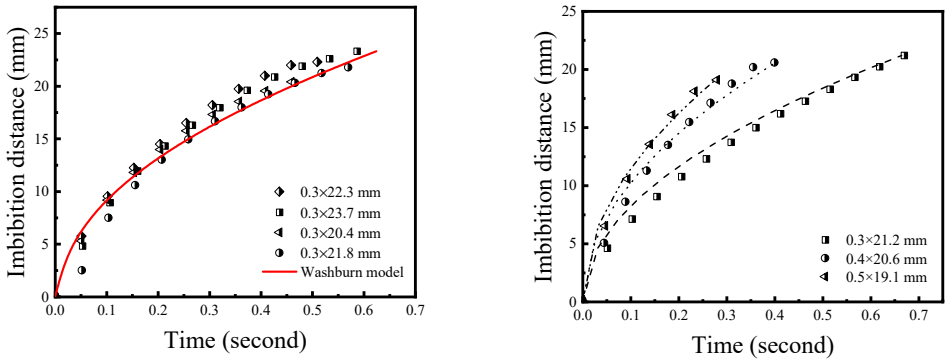

(**a**) (**b**)

Figure 2. Diagram of the imbibition distance as a function of time in imbibition experiments of liquid-displacing-air in circular single channels. ((**a**) shows the experimental results of water-displacing-air, (**b**) shows the experimental results of oil-displacing-air; these curves and point sets represent Washburn model's prediction curves and the experimental results, respectively).

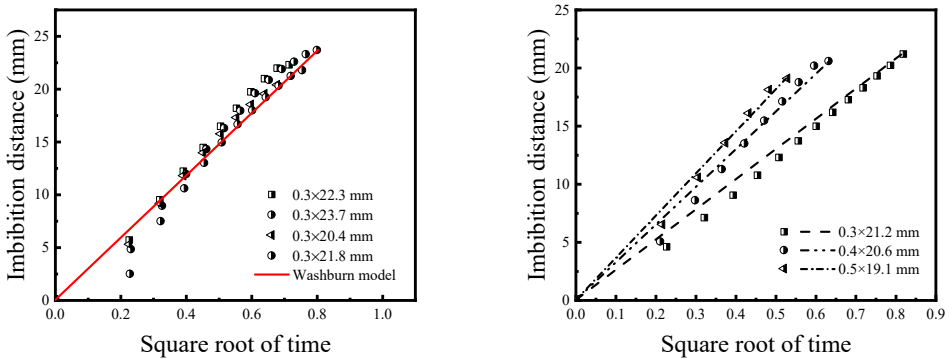

(**a**) (**b**)

Figure 3. Diagram of the imbibition distance as a function of $\sqrt{t}$ in imbibition experiments of liquid-displacing-air in circular single channels. ((**a**) shows the experimental results of water-displacing-air, (**b**) shows the experimental results of oil-displacing-air; these curves and point sets represent Washburn model's prediction curves and the experimental results respectively).

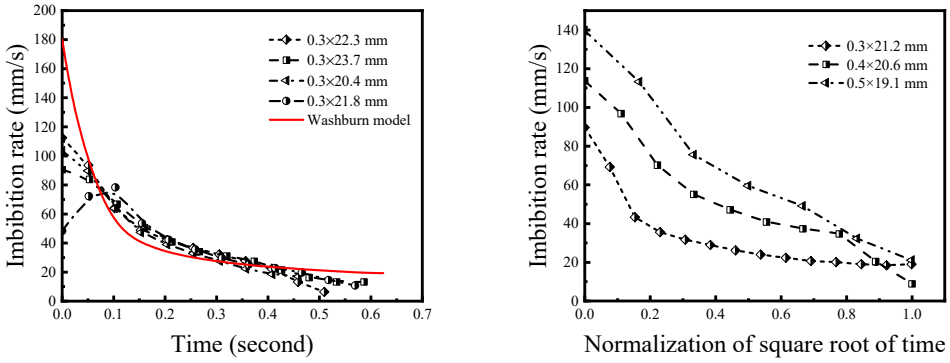

(**a**) (**b**)

Figure 4. Diagram of the imbibition rate as a function of time. ((**a**) shows the experimental results of water-displacing-air, (**b**) shows the experimental results of oil-displacing-air; these curves and point sets represent Washburn model's prediction curves and the experimental results respectively).

Figure 4a shows that imbibition rates obtained from experiments agree well with the Washburn model after 0.1 s. Mismatch within 0.1 s is likely due to the inertial effect when

water (or oil) enters the channel [27]. From the derivation of Equation (1), the capillary force remains unchanged during the whole imbibition process, so the liquid initially imbibed into the single channel produces a great acceleration under the effect of constant capillary force. However, in the actual imbibition process, the velocity of the front in the single channel is affected by the inertance of the DI-water remaining at the inlet.

Figure 4b shows that the tendencies of the imbibition rate, which decrease with time, are the same in different single channels with different diameters in imbibition experiment of oil-displacing-air. In addition, the imbibition rate increases for increased diameters of the single channel, and the increasing rate of imbibition rate reduces with the diameter of the single channel which reflecting that the imbibition rate does not increase infinitely with the increase of tube diameter. The Washburn model predicts such behavior. The good match of Washburn model and experimental results during imbibition of liquid-displacing-air indicates that the wettability of the channel wall remains unchanged during the imbibition.

3.2. Water-Displacing-Oil

Imbibition of a water-displacing-oil is different from that of liquid-displacing-air. As for the former one, the viscosity of the displaced phase can't be neglected. In fact, the model should be modified by introducing the viscosity of the displaced phase, shown in Equation (4). In the imbibition experiments of water-displacing-oil, the focus is to determine how the length and diameter of single channel influence the imbibition behavior, so viscosity of liquid and wettability of channel wall should keep constant. As shown in imbibition experiments of liquid-displacing-air in Table 1 and Figure 3, wettability of the inner wall remains unchanged during imbibition, so is the viscosity of liquid.

The experimental results of the imbibition distance as a function of time in imbibition experiments of water-displacing-oil are obtained through the microfluidic platform, as shown in Figure 5.

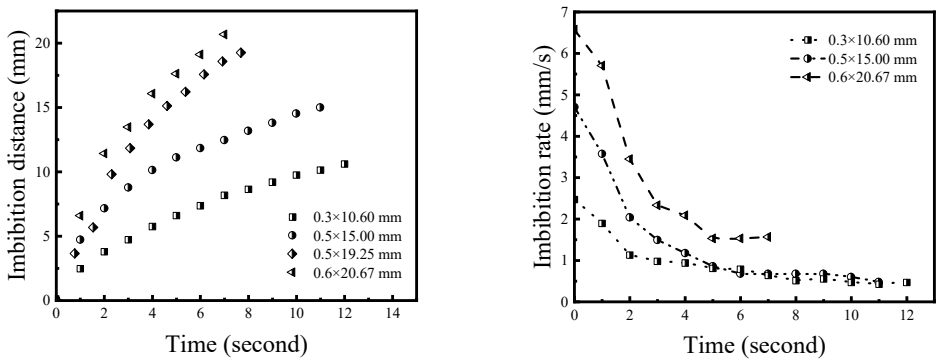

(**a**) (**b**)

Figure 5. (**a**) Diagram of the imbibition distance as a function of time in water-displacing-oil experiments in circular single channels. (**b**) Diagram of the imbibition rate as a function of time. (Three of the four sets of experiment data specified in (**a**) are selected randomly for the subsequent fitting analysis, and the remaining one set of data thereof is for verification on fitting steps, as indicated in (**b**)).

Figure 5 shows that the imbibition rate is in the same tendency in several groups of imbibition experiments in which the lower-viscosity DI-water displaces the higher-viscosity kerosene, that is, the imbibition rate gradually decreases during spontaneous imbibition, and increases with the increase of diameter of single channel, of which the effect on imbibition rate is widely known. Figure 5a also shows that in the single channel with the same diameter, the length has a great influence on imbibition rate, which is caused by the viscosity of displaced phase.

Combined with the parameters in Table 1 and Equation (4), the prediction curve of Poiseuille model in a single channel with diameter of 0.3 mm is drawn, and the result of imbibition experiment and prediction curve are compared, as shown in Figure 6.

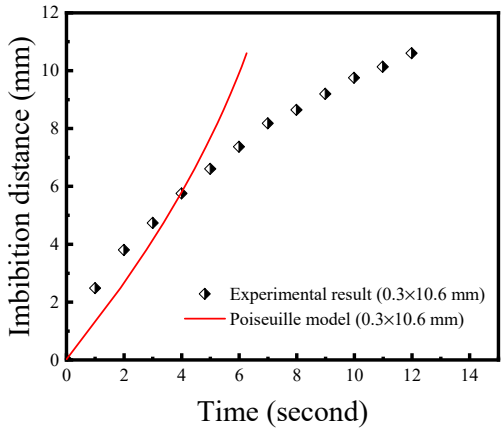

Figure 6. Comparison diagram of experimental data and Poiseuille model curve of imbibition experiments of water-displacing-oil in circular single channel.

Figure 6 shows that curve of the imbibition distance as a function of time obtained by Poiseuille model is different from that of experimental result, which was also observed in Yang's paper [23].

The reasons of this abnormal phenomenon are as follows. In the Poiseuille model it is assumed that displacement force only comes from capillary force at water-oil interface, displacement resistance comes from viscous force generated by flow of oil and water, and other forces are ignored. In the actual core displacement experiment, displacement pressure difference that is far greater than capillary force is applied to the core so that the influence of other displacement resistances on flow can be ignored. Moreover, the imbibition experiments with single-channel model are subject to the trend of imbibition rate in the gradual decrease both in case that the lower-viscosity liquid displaces the higher-viscosity one and the higher-viscosity liquid displaces the lower-viscosity one. While the Equation (4) indicates that such a decreasing trend for imbibition rate is normal when the higher-viscosity liquid displaces the lower-viscosity one. However, the decreasing trend of imbibition rate is abnormal in actual imbibition experiments of the lower-viscosity liquid displacing the higher-viscosity one compared to the increasing trend shown in Equation (4). Therefore, Equation (4) needs to be modified on combination of the actual experimental conditions and specific forces.

In the imbibition experiment of water-displacing-oil, a single channel initially saturated with kerosene is placed on a horizontal glass base, and water droplet is quantitatively dropped at one end of the single channel (inlet end). Water is imbibed into the single channel due to the capillary farce. At the same time, kerosene is displaced from the other end of the single channel (outlet end), and imbibed reversely to the inlet end of the single channel along the angle between the single channel and the horizontal glass base. The reverse imbibition at the outer angle is one kind of imbibition of liquid-displacing-air. Thus, capillary force, viscous force and the force caused by the reverse imbibition are the three main forces.

The mechanism of the third force is as follows. Due to reverse imbibition of kerosene a small concave meniscus will appear at the outlet end of the single channel, and the curvature of concave meniscus decreases with the increase of the volume of kerosene gathered at the angle outside the single channel. During the period of concave meniscus, the force caused by the reverse imbibition stimulates the imbibition of water-displacing-oil inside the single channel. Then, the concave meniscus disappears and transition to a convex meniscus occurs until the kerosene accumulated at the angle reaches the limit volume allowed by wettability. At this moment, the force produced by the reverse imbibition hinders the internal imbibition Therefore, in the imbibition experiment conducted in capillary tubes, displaced phase not only produces a viscous force inside the capillary tube, but also generates an additional force when accumulating outside the tube.

The reverse imbibition is affected by the wettability both of the single channels and the glass base that is one component of the microfluidic platform, all of which determines the liquid storage capacity of the angle outside single channel. The liquid storage capacity is related to the limit volume of concave meniscus. In this study, wettability of glass base and single channels keeps constant, for the glass base is cleaned and dried once an imbibition experiment is completed with it, and every new single channel used for each experiment is provided by the same supplier.

After analyzing the forces, Poiseuille model can be modified by introducing the third force. Therefore, the differential pressure ΔP is modified shown as Equation (7):

$$\Delta P = P_c + P_c' \tag{7}$$

P_c' represents the third force, which is related to imbibition distance.

After introducing the third force, the key is to determine its expression.

According to the specific experimental situation, the following hypothesis is made: the kerosene displaced from the single channel instantly fills the external angle. This is since the imbibition at the angle is a kind of imbibition of liquid-displacing-air, of which the imbibition rate is much higher than that of water-displacing-oil.

From the geometric analysis, it can be known that the shapes of cross section of kerosene gathered at the included angle outside the single channels are similar when the normalized imbibition distances in single channels with different diameters are the same. Moreover, the shape of the cross section is only related to the normalized imbibition distance on premise of the same wettability.

Thus, P_c' can be expressed as follows in Equation (8):

$$P_c' = a \times \left(\frac{L}{L_{channel}}\right)^n + b \tag{8}$$

Therein, a, b and n represent 3 characteristic parameters.

Then, the ultimate expression is shown in Equation (9):

$$\frac{R^2}{8}\left[P_c + a \times \left(\frac{L}{L_{channel}}\right)^n + b\right] \times t = \frac{1}{2}(\mu_w - \mu_{nw})L^2 + \mu_{nw}L_{channel}L \tag{9}$$

According to the analysis in the Appendix A, the value of the characteristic parameter n is 0.5. And then, characteristic parameter a and b need to be determined by following steps.

When the imbibition process is finished, P_c' can be expressed as Equation (10):

$$P_{cend}' = a + b \tag{10}$$

Therein, P_{cend}' indicates the P_c' at the end of imbibition.

According to Equation (9), all parameters other than characteristic parameter a and b are known during the whole imbibition process, so P_{cend}' can be calculated when the imbibition process is finished. P_{cend}' in one experiment is constant, so is the sum of a plus b. Therefore, the optimal fitting curve is obtained by constantly adjusting the values of a and b to fit the experimental data. Finally, characteristic parameters a and b are determined.

Thus, characteristic parameter n, a and b are determined in each imbibition experiment, as shown in Table 2.

Table 2. Values of characteristic parameters a and b.

	0.3 × 10.60 mm	**0.5 × 15.00 mm**	**0.6 × 20.67 mm**
a	−18.50	−21.07	−34.08
b	13.63	14.19	24.12

According to these parameters, the modified curve of Poiseuille model is drawn in Figure 7.

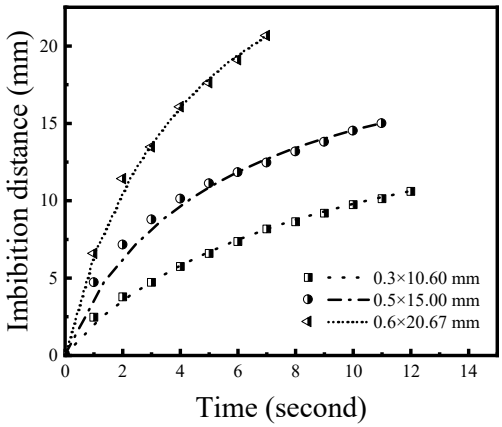

Figure 7. Comparison diagram between the fitted model curves and the corresponding experimental results (These curves represent the modified Poiseuille model curves, and the series of points represent the corresponding experimental data).

Figure 7 shows that the modified Poiseuille model can better reflect the law of imbibition rate in the imbibition process that the lower-viscosity liquid displaces the higher-viscosity liquid.

In the three groups of imbibition experiments of water-displacing-oil above, the prediction curve is adjusted and fitted with the experimental data by changing characteristic parameter a and b, then the best prediction curve is obtained, and the corresponding characteristic parameter a and b are concluded. As a result, all parameters in Equation (9) are known. Furthermore, a constant dimensionless parameter P'_{c0}/P_c (details refer to Table 3), which is consistent with that in other imbibition experiments of water-displacing-oil, is found and used for calculating characteristic parameters a and b.

Table 3. Parameters at the initial and terminal positions of imbibition.

	0.3 × 10.60 mm	**0.5 × 15.00 mm**	**0.6 × 20.67 mm**
P'_{c0} (or b)	13.63	14.19	24.12
P'_{c0}/P_c	1.34	1.28	1.29

(P'_{c0}/P_c represents the ratio of the third force at the angle outside the single channel to the capillary force inside the single channel when t = 0).

In other imbibition experiments under same conditions, characteristic parameter a and b are determined according to the constant dimensionless parameter.

Specific steps are as follows.

When $t = 0$, Equation (8) can be expressed as Equation (11):

$$P'_{c0} = b \tag{11}$$

P'_{c0} and the ratio of P'_{c0} to P_c are calculated and shown in Table 3:

Table 3 shows that the average value of P'_{c0}/P_c is 1.30. Capillary force can be easily calculated, and P'_{c0} can be calculated as well according to the value of P'_{c0}/P_c. Therefore, characteristic parameter b is obtained. In addition, P'_{cend} equal to the sum of a and b is calculated according to Equation (9). Thus, characteristic parameter a is calculated. Upon conclusion of the step above, the Equation (9) utilized in the three imbibition experiments is, respectively, determined.

To verify the practicability and accuracy of this modified Poiseuille model, characteristic parameter a and b in other imbibition experiments of water-displacing-oil are calculated

through the above method, and the parameters used in this verification case include the dimensionless parameter shown in Table 3 and the measured parameters shown in Table 1 and Figure 5. The prediction curve of modified Poiseuille model is obtained, as shown in Figure 8.

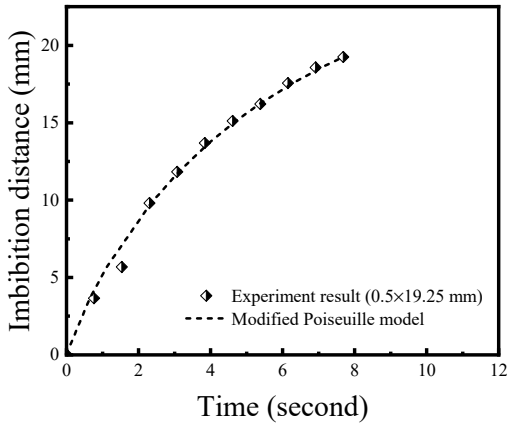

Figure 8. Comparison diagram between the prediction curve of modified Poiseuille model and experimental result in one 0.5 × 19.25 mm single channel. These experiment data are derived from Figure 5a.

Figure 8 shows that the modified Poiseuille model has a good prediction effect. According to the above analysis of imbibition of water-displacing-oil in a single channel, when the viscosity of the displaced phase cannot be ignored, the accumulation effect by the external liquid on imbibition process cannot be ignored as well.

In the modified Poiseuille model, the effects of the length and diameter of the single channel and additional force come from the reverse imbibition on the imbibition are considered. After introducing the additional force called as the third force above, the modified Poiseuille model can describe the imbibition process of water-displacing-oil, which is used to predict the imbibition process where the lower-viscosity liquid displaces the higher-viscosity liquid. The accumulation effect on imbibition in the process that the higher-viscosity liquid displaces the lower-viscosity liquid is likely to exist, and it is ignored for the tendency of imbibition rate is unchanged (although the accumulation effect is considered).

4. Conclusions

In this study, spontaneous imbibition of liquid-displacing-air and water-displacing-oil is respectively observed through the microfluidics. According to the study on the reverse imbibition occurred from the displaced phase at the angle outside single channel, Poiseuille model describing the liquid-liquid spontaneous imbibition is modified.

(1) In experiments of spontaneous imbibition of liquid-displacing-air, the results are in line with Washburn model and match well with previous results using the vapor whose viscosity is significantly lower than the liquid.

(2) The experimental results in the lower-viscosity liquid (DI-water) displacing the higher-viscosity one (kerosene/oil) show that the imbibition rate decreases with time, which is not in line with the increasing trend of imbibition rate indicated in Equation (4).

(3) On the basis of the Poiseuille model, a new model is proposed that includes the additional force from the accumulated fluid flowing out of the single channel. The modified Poiseuille model matches well with the experimental results and shows that a good prediction effect in the water-displacing-oil imbibition experiment.

Author Contributions: Conceptualization, W.D. and T.L.; Data curation, W.D.; Formal analysis, W.D.; Funding acquisition, T.L.; Methodology, W.D.; Supervision, T.L., F.Z. and J.L.; Validation, S.Y.; Writing—original draft, W.D.; Writing—review & editing, T.L. All authors have read and agreed to the published version of the manuscript.

Funding: This research was funded by the Strategic Cooperation Technology Projects of CNPC and CUPB (ZLZX2020-01).

Institutional Review Board Statement: Not applicable.

Informed Consent Statement: Not applicable.

Data Availability Statement: Not applicable.

Acknowledgments: This work was financially supported by the Strategic Cooperation Technology Projects of CNPC and CUPB (ZLZX2020-01).

Conflicts of Interest: The authors declare no conflict of interest.

Appendix A

Characteristic Parameter n

When P_c' is positive, it is obvious that the volume of kerosene accumulated at the angle outside the single channel has not reached the limit of aggregation volume allowed by wettability ($P_c' = 0$), and the displaced kerosene at the angle can also conduct spontaneous imbibition along the outer tube wall. It is assumed to set the capillary force providing spontaneous imbibition at the external angle to P_c''. The larger P_c'' is, the faster the rate of reverse imbibition of kerosene is, the greater the force on internal imbibition of water-displacing-oil is, and the higher the imbibition rate of internal imbibition is. Thus, P_c' and P_c'' change in the same way. Therefore, P_c'' is analyzed to determine the characteristic parameter n that reflects the trend of P_c'.

According to experimental conditions, the shape of cross section of kerosene outside the single channel is shown in Figure A1.

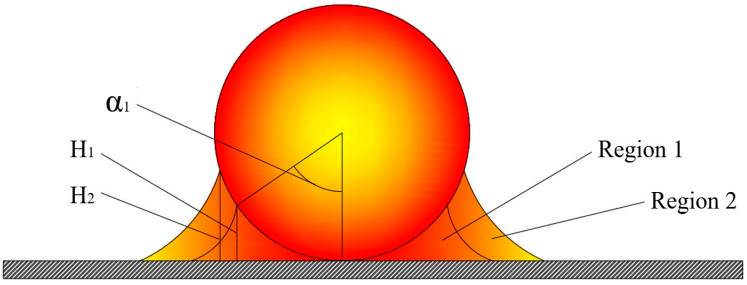

Figure A1. Schematic diagram of the cross section.

Due to the difference between imbibition of liquid-displacing-air and that of water-displacing-oil, the displacement resistance of kerosene-displacing-air is far less than that of water-displacing-oil, so that the outer kerosene is evenly distributed at the angle which named region 1 in a very short time. And then, kerosene is displaced out of the single channel, and reversely imbibed along the angle at region 2. The area of region 1 is equal to the area of region 2. Assuming the imbibition distance inside the single channel is L, the cross-sectional area at the angle is shown in Equation (A1):

$$S = \frac{\pi R^2 \cdot L}{L_{channel}} \tag{A1}$$

As shown in this figure, the height of the cross section of kerosene at the angle corresponding to a certain imbibition distance is H, and the corresponding angle is α. The

contact angle between the external angle and the horizontal base is θ'. Therefore, the cross-sectional area at the angle is also expressed as Equation (A2):

$$S = 2 \times \left[\frac{H^2}{2tan\theta'} + \frac{1}{2}(H + R) \cdot R \cdot sin\alpha - \frac{1}{2} \cdot \frac{\alpha \cdot \pi}{180} \cdot R^2 \right] \tag{A2}$$

The relationship between the height of cross section and the imbibition distance can be obtained by substituting values, as shown in Figure A2.

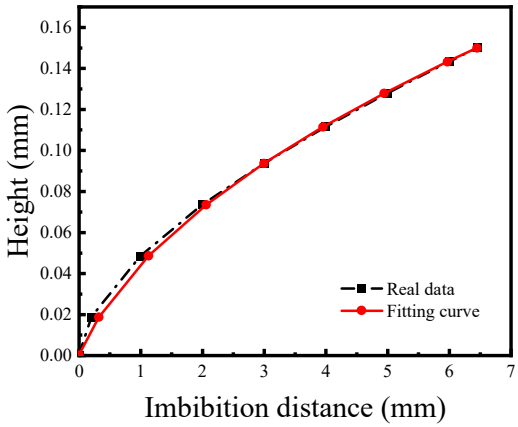

Figure A2. The curves of the height of cross section as a function of imbibition distance (the black curve is obtained according to Equations (A1) and (A2), the red one is a fitting curve).

The expression of the fitting curve is shown in Equation (A3):

$$L = 195.0718 \times H^2 + 13.7926 \times H \tag{A3}$$

This expression reflects the relationship between the imbibition distance in the single channel and the height of the cross-sectional area at the angle outside the single channel.

And then, the relationship between P_c'' and imbibition distance is obtained by analyzing the relationship between P_c'' and H.

Combined with the analysis above, the imbibition rate of water-displacing-oil inside the single channel is far less than that of kerosene-displacing-air at the angle outside the single channel. Therefore, the following assumption is made: when the initial length of water phase imbibed into the single channel is L_0, the kerosene displaced from the outlet end must be imbibed in reverse at a very fast speed and evenly distributed at the external angle (region 1). At this moment, the height of the cross-section at the external angle is H_1. When the water phase is imbibed the second length of L_0, the displaced kerosene will be reversely imbibed at region 2. Therefore, the expression of P_c'' is given as Equation (A4):

$$\begin{cases} P_{c1}'' = \dfrac{2\sigma R \cdot \frac{\alpha_1 \cdot \pi}{180} \cdot cos\theta'' + 2\sigma \cdot \left(\frac{H_1}{tan\theta'} + Rsin\alpha_1 \right) \cdot cos\theta'}{\frac{\pi R^2 L_0}{L_{channel}}} & (k = 1) \\ P_{ck}'' = \dfrac{2\sigma R \cdot (\alpha_k - \alpha_{k-1}) \cdot \frac{\pi}{180} \cdot cos\theta'' + 2\sigma \cdot \left[\frac{H_k - H_{k-1}}{tan\theta'} + R(sin\alpha_k - sin\alpha_{k-1}) \right] \cdot cos\theta'}{\frac{\pi R^2 L_0}{L_{channel}}} & (k > 1) \end{cases} \tag{A4}$$

Therein, k represents the ratio of imbibition distance to L_0; α_k and r_k, respectively, represent the height and angle when the corresponding imbibition distance is $k \cdot L_0$, as shown in Figure A1. θ' represents the contact angle between kerosene and the glass base; θ'' represents the contact angle between kerosene and the outer wall of the single channel.

The height H_k in Equation (A4) can be expressed by imbibition distance L, as shown in Equation (A3). Thus, P_c'' in Equation (A4) is a function of L. The relationship between P_c'' and the imbibition distance (L) is shown in Figure A3.

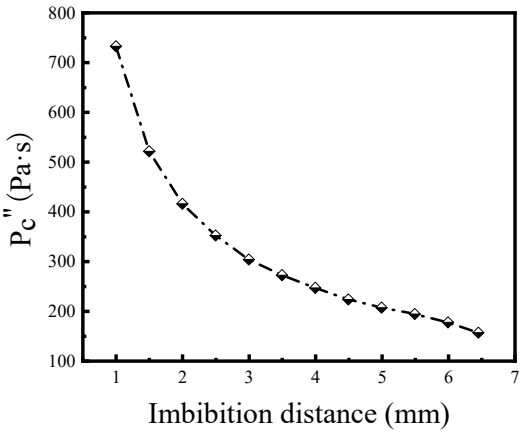

Figure A3. The curve of P_c'' as a function of imbibition distance.

The figure above shows that P_c'' has a linear relationship with the square root of imbibition distance (L), and P_c'' decreases with the increase of imbibition distance, so the characteristic parameter a in Equation (8) is negative. According to the similarity between P_c' and P_c'', the characteristic parameter n in Equation (8) is determined to be 0.5.

Expression (8) and Expression (9) become the following expression as shown in Equations (A5) and (A6):

$$P_c' = a \times \left(\frac{L}{L_{channel}}\right)^{0.5} + b \tag{A5}$$

$$\frac{R^2}{8} \cdot \left[P_c + a \times \left(\frac{L}{L_{channel}}\right)^{0.5} + b\right] \cdot t = \frac{1}{2} \cdot (\mu_w - \mu_{nw}) \cdot L^2 + \mu_{nw} L_{channel} L \tag{A6}$$

Equation (A6) is a modified model considering the third force at the angle outside the single channel. The values of characteristic parameters a and b can be obtained by the curves of time and distance in the imbibition process, and then a modified Poiseuille model for imbibition of water-displacing-oil can be obtained, which can be used to predict the imbibition process under the same conditions.

References

1. Liang, T.; Zhao, X.; Yuan, S.; Zhu, J.; Liang, X.; Li, X.; Zhou, F. Surfactant-EOR in tight oil reservoirs: Current status and a systematic surfactant screening method with field experiments. *J. Pet. Sci. Eng.* **2021**, *196*, 108097. [CrossRef]
2. Sun, L.; Zou, C.; Jia, A.; Wei, Y.; Zhu, R.; Wu, S.; Guo, Z. Development characteristics and orientation of tight oil and gas in China. *Pet. Explor. Dev.* **2019**, *46*, 1073–1087. [CrossRef]
3. Chen, W.; Zhang, Z.; Liu, Q.; Chen, X.; Opoku Appau, P.; Wang, F. Experimental Investigation of Oil Recovery from Tight Sandstone Oil Reservoirs by Pressure Depletion. *Energies* **2018**, *11*, 2667. [CrossRef]
4. Sheng, J.J. What type of surfactants should be used to enhance spontaneous imbibition in shale and tight reservoirs? *J. Pet. Sci. Eng.* **2017**, *159*, 635–643. [CrossRef]
5. Zou, C.; Zhang, G.; Yang, Z.; Tao, S.; Hou, L.; Zhu, R.; Yuan, X.; Ran, Q.; Li, D.; Wang, Z. Concepts, characteristics, potential and technology of unconventional hydrocarbons: On unconventional petroleum geology. *Pet. Explor. Dev.* **2013**, *40*, 413–428. [CrossRef]
6. Mason, G.; Morrow, N.R. Developments in spontaneous imbibition and possibilities for future work. *J. Pet. Sci. Eng.* **2013**, *110*, 268–293. [CrossRef]
7. Lucas, R. Ueber das Zeitgesetz des kapillaren Aufstiegs von Flüssigkeiten. *Kolloid-Zeitschrift* **1918**, *23*, 15–22. [CrossRef]
8. Washburn, E.W. The Dynamics of Capillary Flow. *Phys. Rev.* **1921**, *17*, 273. Available online: https://journals.aps.org/pr/abstract/10.1103/PhysRev.17.273 (accessed on 9 November 2021). [CrossRef]
9. Zhang, J.; Sun, Z.; Wang, X.; Kang, X. Study on the Oil Displacement Effect and Application of Soft Microgel Flooding Technology. In Proceedings of the SPE Middle East Oil & Gas Show and Conference, event canceled, 28 November–1 December 2021.
10. Qin, T.; Fenter, P.; AlOtaibi, M.; Ayirala, S.; AlYousef, A. Pore-Scale Oil Connectivity and Displacement by Controlled-Ionic-Composition Water-flooding Using Synchrotron X-ray Microtomography. *SPE J.* **2021**, *26*, 3694–3701. [CrossRef]
11. Mirzaei-Paiaman, A.; Masihi, M. Scaling Equations for Oil/Gas Recovery from Fractured Porous Media by Counter-Current Spontaneous Imbibition: From Development to Application. *Energy Fuels* **2013**, *27*, 4662–4676. [CrossRef]

12. Wang, F.; Zhao, J. A mathematical model for co-current spontaneous water imbibition into oil-saturated tight sandstone: Up-scaling from pore-scale to core-scale with fractal approach. *J. Pet. Sci. Eng.* **2019**, *178*, 376–388. [CrossRef]
13. Li, C.; Shen, Y.; Ge, H.; Zhang, Y.; Liu, T. Spontaneous imbibition in fractal tortuous micro-nano pores considering dynamic contact angle and slip effect: Phase portrait analysis and analytical solutions. *Sci. Rep.* **2018**, *8*, 3919. [CrossRef] [PubMed]
14. Hilpert, M. Effects of dynamic contact angle on liquid infiltration into horizontal capillary tubes: (Semi)-analytical solutions. *J. Colloid Interface Sci.* **2009**, *337*, 131–137. [CrossRef] [PubMed]
15. Hilpert, M. Effects of dynamic contact angle on liquid infiltration into inclined capillary tubes: (Semi)-analytical solutions. *J. Colloid Interface Sci.* **2009**, *337*, 138–144. [CrossRef]
16. Soares, E.J.; Carvalho, M.S.; Mendes, P.R.S. Immiscible Liquid-Liquid Displacement in Capillary Tubes. *J. Fluids Eng.* **2005**, *127*, 24–31. [CrossRef]
17. Yang, W.; Fu, C.; Du, Y.; Xu, K.; Balhoff, M.T.; Weston, J.; Lu, J. Dynamic Contact Angle Reformulates Pore-Scale Fluid-Fluid Displacement at Ultralow Interfacial Tension. *SPE J.* **2021**, *26*, 1278–1289. [CrossRef]
18. Tian, W.; Wu, K.; Chen, Z.; Lai, L.; Gao, Y.; Li, J. Effect of Dynamic Contact Angle on Spontaneous Capillary-Liquid-Liquid Imbibition by Molecular Kinetic Theory. *SPE J.* **2021**, *26*, 2324–2339. [CrossRef]
19. Sugar, A.; Torrealba, V.; Buttner, U.; Hoteit, H. Assessment of Polymer-Induced Clogging Using Microfluidics. *SPE J.* **2021**, *26*, 3793–3804. [CrossRef]
20. Xu, K.; Liang, T.; Zhu, P.; Qi, P.; Lu, J.; Huh, C.; Balhoff, M. A 2.5-D glass micromodel for investigation of multi-phase flow in porous media. Lab on a Chip. *R. Soc. Chem.* **2017**, *17*, 640–646.
21. Han, A.; Mondin, G.; Hegelbach, N.G.; de Rooij, N.F.; Staufer, U. Filling kinetics of liquids in nanochannels as narrow as 27 nm by capillary force. *J. Colloid Interface Sci.* **2006**, *293*, 151–157. [CrossRef]
22. Yang, L.-J.; Yao, T.-J.; Tai, Y.-C. The marching velocity of the capillary meniscus in a microchannel. *J. Micromech. Microeng.* **2004**, *14*, 220–225. [CrossRef]
23. Yang, D.; Krasowska, M.; Priest, C.; Ralston, J. Dynamics of capillary-driven liquid–liquid displacement in open microchannels. *Phys. Chem. Chem. Phys.* **2014**, *16*, 24473–24478. [CrossRef] [PubMed]
24. Yang, D.; Krasowska, M.; Priest, C.; Popescu, M.N.; Ralston, J. Dynamics of Capillary-Driven Flow in Open Microchannels. *J. Phys. Chem. C* **2011**, *115*, 18761–18769. [CrossRef]
25. Chen, T. Capillary force-driven fluid flow of a wetting liquid in open grooves with different sizes. In *Fourteenth Intersociety Conference on Thermal and Thermomechanical Phenomena in Electronic Systems (ITherm)*; IEEE: Orlando, FL, USA, 2014; pp. 388–396.
26. Deng, Y.; Li, J.; Meng, J.; Cao, Y.; Zhao, L.; Zhao, J. Study on Marine Pipelines Forced Vibration and Vortex-Induced Vibration in Uniform flow and Combined Flow at Different Reynolds Number. In Proceedings of the 31st International Ocean and Polar Engineering Conference, Rhodes, Greece, 20–25 June 2021.
27. Tian, W.T.; Wu, K.; Chen, Z.; Gao, Y.; Gao, Y.; Li, J. Inertial Effect on Spontaneous Oil-Water Imbibition by Molecular Kinetic Theory. In Proceedings of the SPE Europec Featured at 82nd EAGE Conference and Exhibition, Amsterdam, The Netherlands, 18–21 October 2021; The Society of Petroleum Engineers (SPE): Dallas, TX, USA, 2021.